

Black Hole Thermodynamics and Heavy Fermion Metals

E. J. Brynjolfsson,¹⁾ U. H. Danielsson,²⁾ L. Thorlacius,^{1),3)} and T. Zingg^{1),3)}

*1) University of Iceland, Science Institute
Dunhaga 3, IS-107 Reykjavik, Iceland*

*2) Institutionen för fysik och astronomi
Uppsala Universitet, Box 803, SE-751 08 Uppsala, Sweden*

*3) NORDITA, Roslagstullsbacken 23
SE-106 91 Stockholm, Sweden*

*E-mail: erlingbr@hi.is, ulf.danielsson@physics.uu.se, lth@nordita.org,
zingg@nordita.org*

ABSTRACT: Heavy fermion alloys at critical doping typically exhibit non-Fermi-liquid behavior at low temperatures, including a logarithmic or power law rise in the ratio of specific heat to temperature as the temperature is lowered. Anomalous specific heat of this type is also observed in a simple class of gravitational dual models that exhibit anisotropic scaling with dynamical critical exponent $z > 1$.

KEYWORDS: Heavy Fermions, Quantum Critical Points, Gauge-gravity correspondence, Black Holes.

Contents

| | |
|---|-----------|
| 1. Introduction | 1 |
| 2. The holographic model | 3 |
| 3. Charged black branes | 5 |
| 3.1 Field equations for static configurations | 6 |
| 3.2 Exact solutions | 7 |
| 3.3 Numerical solutions | 7 |
| 3.4 Asymptotic behavior at large u | 8 |
| 4. Black brane thermodynamics | 9 |
| 4.1 Scaling at high temperature | 11 |
| 4.2 Low-temperature behavior | 11 |
| 5. Discussion | 13 |

1. Introduction

Heavy fermion systems exhibit very interesting thermodynamic properties at low temperature. The Sommerfeld ratio of the specific heat to temperature at low T is very large in these materials indicating an effective mass for the electrons near the Fermi surface that can be orders of magnitude larger than the free electron mass, hence the term heavy fermions. In low-temperature experiments on certain heavy fermion alloys at critical doping the Sommerfeld ratio does not settle down to a constant, as it would for a conventional Fermi liquid, but continues to rise as the temperature is lowered [1]. This behavior has also been observed in systems at near-critical doping by tuning external parameters such as pressure or magnetic field [1, 2]. The non-Fermi-liquid behavior of the specific heat is attributed to strongly correlated physics, governed by an underlying quantum critical point (see [3, 4, 5] for reviews of heavy fermion systems) but a detailed understanding of quantum critical metals remains a key problem in theoretical physics [6].

The last few years have seen increased interest in developing dual gravity models for strongly interacting systems in condensed matter physics (see [7, 8, 9, 10, 11] for recent reviews). While the gravitational approach has found a number of interesting applications it should be emphasized that its ultimate relevance to real

condensed matter systems remains speculative. The original AdS/CFT conjecture [12], for which there is by now strong evidence, relates maximally supersymmetric 3+1 dimensional Yang-Mills gauge theory with a large number of colors to supergravity on a ten dimensional $\text{AdS}_5 \times \text{S}_5$ spacetime. In condensed matter physics one is instead interested in systems without supersymmetry where the validity of a gravitational dual description is a more open question. Furthermore, the large number of colors plays a key role in the supersymmetric gauge theory context in justifying the use of large-scale classical geometry on the gravitational side of the duality and it is at present unclear what the corresponding formal limit would be for the strongly coupled condensed matter systems that one wants to model. These are important issues to settle but in the present paper we pursue a more modest goal of identifying yet another physical effect that can be phenomenologically modeled by a relatively simple dual gravitational system.

Gravity duals have one or more additional spatial dimensions compared to the field theory in question. Finite temperature effects are studied by having a black hole in the higher-dimensional spacetime and when the black hole is electrically charged the Hawking temperature and the black hole charge provide competing energy scales that can lead to interesting dynamics. We will consider quantum critical points in three spatial dimensions that are characterized by a scaling law,

$$t \rightarrow \lambda^z t, \quad \vec{x} \rightarrow \lambda \vec{x}, \quad (1.1)$$

where the dynamical critical exponent z is in general different from 1. We are particularly interested in quantum phase transitions in heavy fermion alloys where the metal goes from being paramagnetic to being antiferromagnetic as the level of doping or some other external control parameter is varied [1, 2]. Theoretical work based on a lattice Kondo model suggests that the associated quantum critical point exhibits anisotropic scaling with a non-universal dynamical critical exponent that can be fitted by comparison to experimental data [13]. In particular, it was found that $z \approx 2.7$ for the critically doped heavy fermion alloy $\text{CeCu}_{5.9}\text{Au}_{0.1}$, whose anomalous specific heat was reported in [1].

In [14] it was conjectured that a strongly coupled system at a fixed point governed by anisotropic scaling of this form could be modeled by a gravity theory in a so called Lifshitz spacetime with the metric,¹

$$ds^2 = L^2 \left(-r^{2z} dt^2 + r^2 d\vec{x}^2 + \frac{dr^2}{r^2} \right), \quad (1.2)$$

which is invariant under the transformation

$$t \rightarrow \lambda^z t, \quad \vec{x} \rightarrow \lambda \vec{x}, \quad r \rightarrow \frac{r}{\lambda}. \quad (1.3)$$

¹See [15] for early work on gravitational backgrounds with anisotropic scaling.

Here L is a characteristic length scale, which will determine the magnitude of the negative cosmological constant in the gravity model, and (t, \vec{x}, r) are dimensionless coordinates in the higher dimensional spacetime. The finite temperature physics of such a system is then encoded into the geometry of a black hole, which is asymptotic to the Lifshitz spacetime (1.2).

In this paper we continue our study of asymptotically Lifshitz black holes from [16, 17] placing an emphasis on their thermodynamic properties. We compute the specific heat of charged asymptotically Lifshitz black holes as a function of temperature, keeping the charge density in the dual field theory fixed. At high T the thermodynamic behavior of the dual system is governed by the symmetries of the quantum critical point leading to a temperature dependence of the specific heat of the form $C \sim T^{3/z}$. This is a direct consequence of scaling and we find the same result in the gravity dual using black hole thermodynamics.

At low T , we observe a crossover in the black hole thermodynamics indicating non-trivial collective effects in the dual field theory. For $z = 1$ our system reduces to the thermodynamics of the well-known AdS-RN black branes. In this case, the specific heat divided by T goes to a constant value in the limit of low temperature, which is the same behavior as seen in a conventional Fermi liquid. This result was obtained previously in [18], where it was interpreted as evidence for the presence of a Fermi surface in the dual system. It was noted in [18], however, from a holographic computation of transport properties that the low-energy effective theory near the Fermi surface cannot be that of weakly interacting fermions. Non-Fermi-liquid behavior has also been observed in spectral functions of probe fermions coupled to the $z = 1$ system [19, 20].

For a non-trivial dynamical critical exponent $z > 1$ the black brane thermodynamics calculation is more involved and we have to rely more heavily on numerical computations. Interestingly, we find qualitatively different behavior in this case. The Sommerfeld ratio C/T now continues to rise as we go to lower temperatures, which is indeed the behavior observed in critically doped heavy fermion systems. The ability of gravity models with Lifshitz scaling to capture this non-Fermi-liquid aspect of real quantum critical metals is interesting and is the main result of the present paper.

2. The holographic model

The application that we have in mind involves a dual field theory in three spatial dimensions and accordingly the gravity dual is defined on a 4+1 dimensional spacetime to accommodate an emergent extra dimension. Most of our results carry over to other dimensions in a straightforward fashion. In particular, similar conclusions can be drawn about planar systems with $d = 2$.

We work with a 4 + 1 dimensional version of the holographic model of Kachru *et al.* [14], as formulated by Taylor [21], and with a Maxwell gauge field added, as

in [17]. The bulk classical action for the gravitational sector consists of two parts,

$$S = S_{\text{Einstein-Maxwell}} + S_{\text{Lifshitz}}. \quad (2.1)$$

The first term is the usual action of 4 + 1 dimensional Einstein-Maxwell gravity with a negative cosmological constant,

$$S_{\text{Einstein-Maxwell}} = \int d^5x \sqrt{-g} \left(R - 2\Lambda - \frac{1}{4} F_{\mu\nu} F^{\mu\nu} \right). \quad (2.2)$$

This is followed by a term involving a massive vector field,

$$S_{\text{Lifshitz}} = - \int d^5x \sqrt{-g} \left(\frac{1}{4} \mathcal{F}_{\mu\nu} \mathcal{F}^{\mu\nu} + \frac{c^2}{2} \mathcal{A}_\mu \mathcal{A}^\mu \right), \quad (2.3)$$

whose sole purpose is to provide backgrounds with anisotropic scaling of the form (1.3). We refer to this auxiliary vector field, which only couples to gravity, as the Lifshitz vector field. The original gravity model of [14] was 3+1-dimensional and anisotropic scaling was obtained by including a pair of coupled two- and three-form field strengths. Upon integrating out the three-form field strength, the remaining two-form becomes a field strength of a massive vector and in this form the model is easily extended to general dimensions [21].

The equations of motion obtained from the action (2.1) consist of the Einstein equations, the Maxwell equations, and field equations for the Lifshitz vector,

$$G_{\mu\nu} + \Lambda g_{\mu\nu} = T_{\mu\nu}^{\text{Maxwell}} + T_{\mu\nu}^{\text{Lifshitz}}, \quad (2.4)$$

$$\nabla_\nu F^{\nu\mu} = 0, \quad (2.5)$$

$$\nabla_\nu \mathcal{F}^{\nu\mu} = c^2 \mathcal{A}^\mu, \quad (2.6)$$

with the energy momentum tensors of the Maxwell and Lifshitz vector fields given by

$$T_{\mu\nu}^{\text{Maxwell}} = \frac{1}{2} (F_{\mu\lambda} F_\nu^\lambda - \frac{1}{4} g_{\mu\nu} F_{\lambda\sigma} F^{\lambda\sigma}), \quad (2.7)$$

$$T_{\mu\nu}^{\text{Lifshitz}} = \frac{1}{2} (\mathcal{F}_{\mu\lambda} \mathcal{F}_\nu^\lambda - \frac{1}{4} g_{\mu\nu} \mathcal{F}_{\lambda\sigma} \mathcal{F}^{\lambda\sigma}) + \frac{c^2}{2} (\mathcal{A}_\mu \mathcal{A}_\nu - \frac{1}{2} g_{\mu\nu} \mathcal{A}_\lambda \mathcal{A}^\lambda). \quad (2.8)$$

The Lifshitz fixed point geometry (1.2) is a solution of the equations of motion provided the characteristic length scale L is related to the cosmological constant Λ via

$$\Lambda = -\frac{z^2 + 2z + 9}{2L^2}, \quad (2.9)$$

the mass of the Lifshitz vector field is fine-tuned to $c = \sqrt{3z}/L$, and the Lifshitz vector field has the background value

$$\mathcal{A}_t = \sqrt{\frac{2(z-1)}{z}} L r^z, \quad \mathcal{A}_{x_i} = \mathcal{A}_r = 0. \quad (2.10)$$

The Maxwell field vanishes in the Lifshitz background, $A_\mu = 0$.

Although we do not do it here, it is straightforward to couple matter to this system. Including a scalar field, for instance, leads to an instability at low T giving rise to holographic superconductors with Lifshitz scaling [17]. It is also interesting to include a coupling to a bulk Dirac spinor and obtain fermion spectral functions along the lines of [19, 20, 22]. We find that the spectral functions in the $z > 1$ theory exhibit many of the same features as in the asymptotically AdS bulk spacetime considered in these earlier works, including peaks at certain values of momentum and frequency, but there are also important differences. In particular, the would be quasiparticle peaks are less sharply defined than their $z = 1$ counterparts.²

3. Charged black branes

In order to study finite temperature effects in the dual strongly coupled field theory we look for static black brane solutions of the equations of motion (2.4) - (2.6) which are asymptotic to the Lifshitz fixed point solution (1.2). We consider a 4+1 dimensional metric of the form

$$ds^2 = L^2 \left(-r^{2z} f(r)^2 dt^2 + r^2 d\vec{x}^2 + \frac{g(r)^2}{r^2} dr^2 \right), \quad (3.1)$$

for which the non-vanishing components of the vielbein can be taken to be

$$e_t^0 = L r^z f(r), \quad e_{x_1}^1 = \dots = e_{x_3}^3 = L r, \quad e_r^4 = L \frac{g(r)}{r}. \quad (3.2)$$

An asymptotically Lifshitz black brane with a non-degenerate horizon has a simple zero of both $f(r)^2$ and $g(r)^{-2}$ at the horizon, which we take to be at $r = r_0$, and $f(r), g(r) \rightarrow 1$ as $r \rightarrow \infty$. It is straightforward to generalize this ansatz to include black holes with a spherical horizon or topological black holes with a hyperbolic horizon but it is the flat horizon case (3.1) that is of direct interest for the gravitational dual description of a strongly coupled 3 + 1 dimensional field theoretic system.

In a static electrically charged black brane background the Maxwell gauge field and the Lifshitz vector can be chosen to be of the form

$$A_M = \{\alpha(r), 0, \dots, 0\}; \quad \mathcal{A}_M = \sqrt{\frac{2(z-1)}{z}} \{a(r), 0, \dots, 0\}, \quad (3.3)$$

where the corresponding coordinate frame components are given by $A_\mu = e_\mu^M A_M$ and $\mathcal{A}_\mu = e_\mu^M \mathcal{A}_M$.

²Work in progress.

3.1 Field equations for static configurations

The Maxwell equations and the equations of motion for the Lifshitz vector can be written in first-order form,

$$\frac{r}{f} \frac{d}{dr} (f \alpha) = -z \alpha + g \beta, \quad (3.4)$$

$$r \frac{d}{dr} (r^3 \beta) = 0, \quad (3.5)$$

$$\frac{r}{f} \frac{d}{dr} (f a) = -z a + z g b, \quad (3.6)$$

$$r \frac{d}{dr} (r^3 b) = 3r^3 g a, \quad (3.7)$$

where β and b are defined via (3.4) and (3.6) respectively. The Maxwell equation (3.5) trivially integrates to

$$\beta(r) = \frac{\rho}{r^3}, \quad (3.8)$$

where the integration constant ρ is proportional to the world-volume electric charge density of the black brane, which in turn is identified with the charge density in the dual field theory by the standard AdS/CFT dictionary [23, 24], as explained in detail in [25].

The Einstein equations reduce to the following pair of first-order differential equations

$$\frac{r}{g} \frac{dg}{dr} = \frac{g^2}{3} \left[\frac{(z-1)}{2} (3a^2 + zb^2) - \frac{(z^2 + 2z + 9)}{2} + \frac{\rho^2}{4r^6} \right] + 2, \quad (3.9)$$

$$\frac{r}{f} \frac{df}{dr} = \frac{g^2}{3} \left[\frac{(z-1)}{2} (3a^2 - zb^2) + \frac{(z^2 + 2z + 9)}{2} - \frac{\rho^2}{4r^6} \right] - z - 1. \quad (3.10)$$

The Lifshitz fixed point solution is given by $\alpha = \rho = 0$ and $f = g = a = b = 1$.

To bring out the underlying scale invariance of the model we rewrite the field equations using $u = \log(r/r_0)$ instead of r and introduce the scale invariant ratio $\tilde{\rho} \equiv \rho/r_0^d$. The remaining Maxwell equation (3.4) and the equations of motion of the Lifshitz field (3.6) and (3.7) reduce to

$$\dot{\alpha} + \frac{\dot{f}}{f} \alpha = -z \alpha + \tilde{\rho} e^{-3u} g, \quad (3.11)$$

$$\dot{a} + \frac{\dot{f}}{f} a = -z a + z g b, \quad (3.12)$$

$$\dot{b} = -3b + 3g a, \quad (3.13)$$

where $\dot{\cdot} \equiv \frac{d}{du}$. The Einstein equations (3.9) and (3.10) can similarly be rewritten

$$\frac{\dot{g}}{g} = \frac{g^2}{6} \left[(z-1) (3a^2 + zb^2) + \frac{\tilde{\rho}^2}{2} e^{-6u} - (z^2 + 2z + 9) \right] + 2, \quad (3.14)$$

$$\frac{\dot{f}}{f} = \frac{g^2}{6} \left[(z-1) (3a^2 - zb^2) - \frac{\tilde{\rho}^2}{2} e^{-6u} + (z^2 + 2z + 9) \right] - z - 1. \quad (3.15)$$

Using these variables, the field equations are manifestly invariant under the rescaling (1.3). For given $z \geq 1$, there is a one parameter family of black brane solutions, labelled by $\tilde{\rho}$. A neutral black brane has $\tilde{\rho} = 0$ while the extremal limit is given by $|\tilde{\rho}| \rightarrow \sqrt{2(z^2 + 2z + 9)}$.

3.2 Exact solutions

When $z = 1$ the terms involving a and b on the right hand side of the Einstein equations drop out. The equations then reduce to those of Einstein-Maxwell theory with a negative cosmological constant and one finds the AdS-RN solution describing charged black branes in $4 + 1$ dimensional asymptotically AdS spacetime,

$$f^2 = \frac{1}{g^2} = (1 - e^{-2u}) \left(1 + e^{-2u} - \frac{\tilde{\rho}^2}{12} e^{-4u} \right), \quad (3.16)$$

$$A_t = \frac{Lr_0\tilde{\rho}}{2} (1 - e^{-2u}). \quad (3.17)$$

At $z > 1$ there is a corresponding family of charged asymptotically Lifshitz black branes. In general these solutions can only be obtained numerically, but it turns out that in the special case $z = 6$ an isolated exact solution can be found [17, 26],

$$b = 1, \quad f^2 = \frac{1}{g^2} = a^2 = 1 - e^{-6u}, \quad A_t = \pm\sqrt{2}Lr_0^6 (e^{3u} - 1). \quad (3.18)$$

We will primarily rely on numerical solutions in the following but the AdS-RN solution and the exact $z = 6$ solution are useful for checking the numerics.

3.3 Numerical solutions

The family of black brane solutions at generic $z > 1$ can be mapped out using numerical techniques similar to those of [16]. The numerical integration is started near the black hole, with suitable boundary conditions for a regular non-degenerate horizon at $u = 0$, and then proceeds outwards towards the asymptotic region. First of all, there should be a simple zero of f^2 and g^{-2} at the horizon. Furthermore, the product $f\alpha$ must have a simple zero at the horizon in order for the gauge connection to be regular there. Similarly, the combination ga on the right hand side of (3.13) should be regular at the horizon and it then follows from (3.12) that b takes a finite value there. Putting all of this together we find that the near-horizon behavior can be parametrized as follows

$$f(u) = \sqrt{u}(f_0 + f_1u + f_2u^2 + \dots), \quad (3.19)$$

$$g(u) = \frac{1}{\sqrt{u}}(g_0 + g_1u + g_2u^2 + \dots), \quad (3.20)$$

$$\alpha(u) = \sqrt{u}(\alpha_0 + \alpha_1u + \alpha_2u^2 + \dots), \quad (3.21)$$

$$a(u) = \sqrt{u}(a_0 + a_1u + a_2u^2 + \dots), \quad (3.22)$$

$$b(u) = b_0 + b_1u + b_2u^2 + \dots \quad (3.23)$$

Inserting these near-horizon expansions into the equations of motion we obtain a two-parameter family of initial value data for any given z , parametrized for instance by $\tilde{\rho}$ and b_0 . It turns out, however, that these two parameters cannot be varied independently but are restricted by the condition that the metric and Lifshitz vector approach the Lifshitz fixed point solution (1.2) and (2.10) sufficiently rapidly as $u \rightarrow \infty$ [16, 27, 28]. This means that for a given value of z the parameter $\tilde{\rho}$ uniquely determines a charged black brane solution, up to overall scale.

3.4 Asymptotic behavior at large u

We now consider the asymptotic behavior of our fields as $u \rightarrow \infty$. The first observation is that the system of equations (3.11) - (3.15) only contains the combination $\frac{\dot{f}}{f}$ and therefore a uniform rescaling of f is a symmetry of the equations. The symmetry is fixed, however, in an asymptotically Lifshitz solution for which $f \rightarrow 1$ as $u \rightarrow \infty$.³

We next observe that (3.15) can be used to eliminate f from (3.12) - (3.14) leaving a closed system of first-order equations for a , b , and g . The large u behavior can be obtained by linearizing around the Lifshitz fixed point $a = b = g = 1$. The corresponding problem for $d = 2$ was discussed in [16, 27] and we omit the details here. At large u , solutions of the full non-linear system approach a linear combination of the eigenmodes of the linearized system plus a universal mode coming from source terms involving $\tilde{\rho}^2$. The leading large u behavior of the eigenmodes is $O(e^{\lambda_i u})$ with the eigenvalues $\lambda_i \in \{-3 - z, \frac{1}{2}(-3 - z \pm \sqrt{9z^2 - 26z + 33})\}$ while the universal mode falls off as $O(e^{-6u})$ independent of z .

Figure 1 shows the three eigenvalues as a function of z . The eigenmode that belongs to the largest eigenvalue is problematic [16, 27, 28]. For $z \geq 3$ it is non-negative and a solution that contains it fails to be asymptotically Lifshitz. For $1 < z < 3$ it is a negative mode but the falloff at large u is too slow to give finite energy. This mode is eliminated in our black hole solutions by fine-tuning the value of b at the black hole horizon. For $z < 3$ the universal e^{-6u} mode is sub-leading compared to the two remaining eigenmodes of the linearized system but at $z > 3$ it dominates the asymptotic behavior. In the dividing $z = 3$ case the linearized system is degenerate and the asymptotic behavior includes powers of u on top of the e^{-6u} falloff.

Finally, we turn to equation (3.11) for the Maxwell field. In the Lifshitz back-

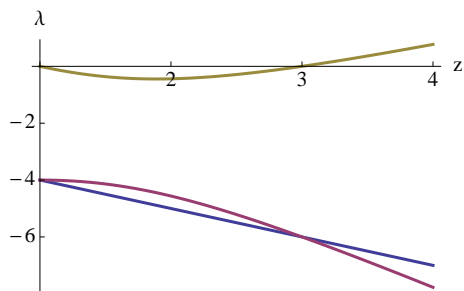


Figure 1: Eigenvalues of the linearized problem for $\{g, b, a\}$ as a function of z for $d = 3$.

³When solving the equations numerically, it is convenient to initially put $f_0 = 1$ in the near-horizon expansion (3.19) when setting up the numerical integration and then rescale f at the end of the day so that $f \rightarrow 1$ as $u \rightarrow \infty$.

ground with $f = g = 1$ it has the solution

$$\alpha = \begin{cases} \tilde{\mu} e^{-zu} + \frac{\tilde{\rho}}{(z-3)} e^{-3u} & \text{if } z \neq 3, \\ \tilde{\mu} e^{-3u} + \tilde{\rho} u e^{-3u} & \text{if } z = 3. \end{cases} \quad (3.24)$$

The non-vanishing component of the vector potential in a coordinate frame is then

$$A_t = \begin{cases} \mu + \frac{L\rho}{(z-3)} r^{z-3} & \text{if } z \neq 3, \\ \mu + L\rho \log\left(\frac{r}{r_0}\right) & \text{if } z = 3, \end{cases} \quad (3.25)$$

with $\mu = L\tilde{\mu}r_0^z$. Once again the qualitative behavior of solutions changes at $z = 3$. For low z values, in the range $1 < z < 3$, the term involving the chemical potential μ dominates compared to the term involving the charge density ρ at large r , while at $z \geq 3$ it is the charge density term that is leading [29].

In general, we are not working with Lifshitz background itself but with solutions of the full non-linear system of equations that are only asymptotically Lifshitz. It turns out, however, the leading large u behavior of α carries over from the Lifshitz background to more general case as long as the value of z isn't too high.⁴

4. Black brane thermodynamics

So far, we have set up the holographic model and considered charged black brane geometries that are conjectured to provide a dual description of a strongly coupled 3+1 dimensional system near a quantum critical point with dynamical critical exponent $z \geq 1$. These black branes turn out to have interesting thermodynamics. At high temperature the thermodynamic behavior is governed by the underlying Lifshitz symmetry, but collective effects come into play as the temperature is lowered and modify the thermodynamics. To see this, we use a combination of analytic and numerical arguments to compute the specific heat of the system as a function of temperature. Our starting point is the following expression for the Hawking temperature of a black brane,⁵

$$T_H = \frac{r_0^z}{4\pi} \frac{f_0}{g_0}, \quad (4.1)$$

which is obtained in the standard way by requiring the Euclidean metric of the black brane to be smooth at the horizon at $r = r_0$. The coefficients f_0 and g_0 are taken from the near-horizon expansions (3.19) and (3.20) in the scale invariant variable u

⁴At $z \geq 9$ we expect non-linear effects to give rise to additional terms in (3.24) with a falloff in between that of the charge density and chemical potential terms. We will not keep track of such terms here since all systems of physical interest that we are aware of have $z < 9$.

⁵From here on we fix the characteristic length scale as $L = 1$. Explicit factors of L can be reintroduced into the formulas by dimensional analysis.

and only depend on the value of $\tilde{\rho}$. The temperature can therefore be expressed as follows,

$$T_H = \frac{r_0^z}{4\pi} F_z(\tilde{\rho}), \quad (4.2)$$

with $F_z(\tilde{\rho}) \equiv \frac{f_0}{g_0}$ for different values of z shown in Figure 2.

The specific heat at fixed volume in the boundary theory is then

$$C = T \frac{dS}{dT} = T \frac{(dS/dr_0)}{(dT/dr_0)}, \quad (4.3)$$

where $S = \frac{1}{4}r_0^3$ is the Bekenstein-Hawking entropy density of the black brane and T in the boundary system is identified with the Hawking temperature (4.2). We have to make a choice whether to work at fixed charge density ρ or fixed chemical potential μ in the boundary theory when calculating thermodynamic quantities. For the field theory problem that we wish to model it is natural to keep the charge density fixed since the net density of charge carriers is given by the density of dopants, which is fixed in a given sample [29]. In this case

$$\frac{d}{dr_0} = \frac{\partial}{\partial r_0} - \frac{3\tilde{\rho}}{r_0} \frac{\partial}{\partial \tilde{\rho}}, \quad (4.4)$$

and we find

$$\frac{C}{T} = \frac{3\pi r_0^{3-z}}{zF_z(\tilde{\rho}) - 3\tilde{\rho}F'_z(\tilde{\rho})}. \quad (4.5)$$

If we instead were to keep the chemical potential μ fixed then

$$\frac{d}{dr_0} = \frac{\partial}{\partial r_0} - \frac{z\tilde{\mu}}{r_0} \left(\frac{d\tilde{\mu}}{d\tilde{\rho}} \right)^{-1} \frac{\partial}{\partial \tilde{\rho}}, \quad (4.6)$$

with $d\tilde{\mu}/d\tilde{\rho}$ obtained from the asymptotic behavior of the Maxwell field (3.24) in the numerical black brane solution, and then the remaining steps in the calculation of the specific heat are parallel to those at fixed charge density.

The variables r_0 and $\tilde{\rho}$ on the right hand side of equation (4.5) refer to the 4+1 dimensional black brane geometry while it is T and ρ that have direct interpretation in the dual field theory. The latter variables are expressed in terms of the former via the definition $\tilde{\rho} = \rho/r_0^3$ and equation (4.2) for the Hawking temperature. We can numerically invert these relations in order to express the specific heat (4.3) in terms T and ρ . Figure 3 shows the map between brane variables and physical variables for $z = 2$ and similar maps are obtained for other z values.

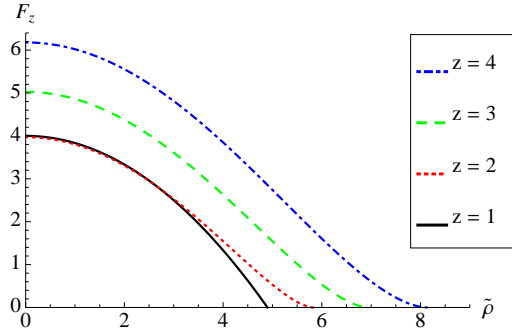


Figure 2: Temperature function $F_z(\tilde{\rho})$ for several z values. The $z = 1$ curve plots the exact result (4.10) while the $z > 1$ curves are obtained from numerical black hole solutions.

4.1 Scaling at high temperature

Below, we present numerical results for C/T obtained via the above procedure for several values of z but some information can be obtained by analytic arguments. In particular, we can extract a scaling relation for the specific heat at high temperature. The argument is the same for any number of spatial dimensions d . Writing $\tilde{\rho} = \rho/r_0^d$, the expression (4.1) for the temperature remains the same except that the detailed shape of the function $F_z(\tilde{\rho})$

depends on d . The limit of high temperature at fixed ρ corresponds to large r_0 and $\tilde{\rho} \rightarrow 0$. The field equations depend on $\tilde{\rho}^2$ in a smooth way so we expect $F_z(\tilde{\rho})$ to be a smooth even function of $\tilde{\rho}$ (this is also evident from the graphs in Figure 2) and the denominator in the d dimensional version of equation (4.5) reduces to $zF_z(0)$. As a result the temperature and the entropy density, and their first derivatives, depend only on the overall scale r_0 in the high-temperature limit and the electric charge carried by the black brane does not affect the dynamics to leading order,

$$T \approx \frac{F_z(0)}{4\pi} r_0^z, \quad S = \frac{1}{4} r_0^d. \quad (4.7)$$

The high-temperature behavior of the specific heat then immediately follows from the general expression (4.3),

$$C \sim r_0^d \sim T^{d/z}, \quad (4.8)$$

which reduces, in particular, to $C \sim T^{3/z}$ when $d = 3$. It is straightforward to go a step further and integrate both sides of (4.3) with respect to T to obtain the following relation between energy and entropy of the system in the high-temperature limit,

$$E = \frac{d}{d+z} T S, \quad (4.9)$$

recovering the result found previously for electrically neutral black branes in [30]. The scaling behavior can be traced to the underlying Lifshitz symmetry of the quantum critical theory. It is easy to see that a generic statistical mechanical system in three spatial dimensions with a dispersion relation of the form $\omega \sim k^z$ exhibits the same scaling behavior [30].

4.2 Low-temperature behavior

At low temperature, the black brane thermodynamics exhibits interesting behavior due to collective effects in the dual field theory and the simple scaling that is seen

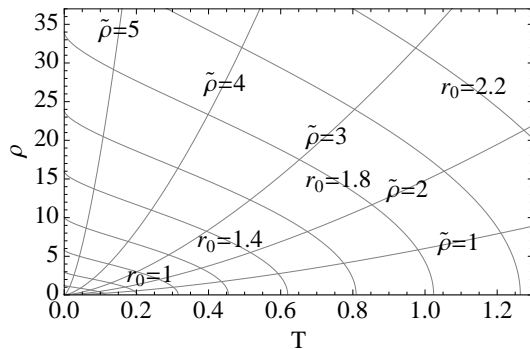


Figure 3: Contour map expressing r_0 and $\tilde{\rho}$ in terms of T and ρ at $z = 2$.

at high temperature no longer applies. The behavior is qualitatively different in conformal systems with $z = 1$ as compared to Lifshitz systems with $z > 1$ and we consider these cases in turn.

At $z = 1$ we have the exact AdS-RN black brane solution (3.17) for which the Hawking temperature is easily determined. One finds

$$F_1(\tilde{\rho}) = 4 - \frac{\tilde{\rho}^2}{6}, \quad (4.10)$$

and the specific heat at fixed ρ is given by

$$\frac{C}{T} = \frac{18\pi r_0^2}{24 + 5\tilde{\rho}^2}. \quad (4.11)$$

At low temperature the charge on the black brane approaches the extremal limit, $\tilde{\rho} \rightarrow \sqrt{24}$ and the specific heat depends linearly on temperature,

$$\frac{C}{T} \rightarrow \frac{\pi\rho^{2/3}}{16 \cdot 3^{1/3}} \quad \text{as } T \rightarrow 0. \quad (4.12)$$

A weakly-coupled Fermi liquid has a specific heat that is linear in T at low temperatures and it is interesting to see the same behavior emerge in the low-temperature limit of a black brane in Einstein-Maxwell theory without having made any reference to specific matter fields in the calculation. This result was obtained previously in [18] where it was taken as evidence for the existence of a Fermi surface in the dual field theory. Spectral functions of probe fermions coupled to the $z = 1$ system computed in [19, 20, 22] also strongly suggest the presence of a Fermi surface. Having a specific heat that is linear in T and a Fermi surface does not imply that the system consists of weakly coupled fermions. Indeed, the scaling behavior of excitations near the Fermi surface differs from that of a Landau Fermi liquid in the probe fermion analysis of [19, 20] and the zero-temperature conductivity computed in [18] was found to be diffusive rather than ballistic, suggesting that disorder plays a role.

At $z > 1$ we do not have explicit analytic black brane solutions except the isolated $z = 6$ solution (3.18) and our results for the specific heat in $z > 1$ systems are therefore based on numerical black brane solutions with non-vanishing Lifshitz vector field. The key qualitative difference compared to the $z = 1$ case can be seen in Figure 2. The function $F_1(\tilde{\rho})$ goes to zero in a linear fashion in the extremal limit $\tilde{\rho} \rightarrow \sqrt{24}$ but for $z > 1$ both $F_z(\tilde{\rho})$ and its first derivative go to zero in the extremal limit $\tilde{\rho} \rightarrow \sqrt{2(z^2 + 2z + 9)}$. It then follows from equation (4.5) that the ratio C/T diverges in the $T \rightarrow 0$ limit for $z > 1$. The growth in C/T towards lower temperatures is evident in the $z > 1$ curves in Figure 4.⁶ This trend is in qualitative agreement with the measured specific heat of certain heavy fermion alloys [4]. The high T behavior of the specific heat curves in the figure, on the other hand, matches the scaling law (4.8).

⁶Finite numerical precision limits how far the curves for $z > 1$ in Figure 4 can be extended towards low T .

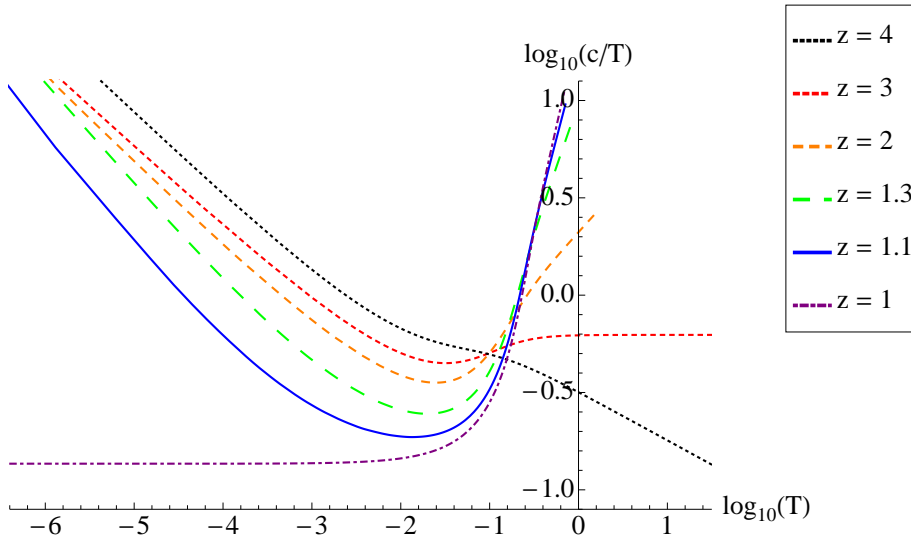


Figure 4: Black brane specific heat divided by temperature for several z values calculated at fixed charged density $\rho = 1$. The $z = 1$ curve is obtained from the exact result (4.11).

5. Discussion

In this paper we have employed a relatively simple holographic description of a strongly coupled 3+1 dimensional quantum critical point with asymmetric scaling to model the anomalous specific heat found at low temperature in many heavy fermion compounds. The calculation is performed entirely within the context of black hole thermodynamics and the nature of the low-lying spectrum of excitations is thus investigated without introducing any specific matter probes. It would be very interesting to complement the results obtained here by a study of spectral functions for probe fermions, generalizing the $z = 1$ work of [19, 20, 22], and a calculation of conductivities. This requires us to extend existing gravitational techniques for obtaining spectral functions and transport coefficients to models exhibiting Lifshitz scaling with non-trivial dynamical critical exponent $z > 1$, and our work in this direction is in progress.

One limitation of the present work concerns the non-vanishing black hole area in the extremal limit, which corresponds to having non-vanishing entropy at zero temperature in the dual system. This can for instance be remedied by coupling the system to a scalar field and include the back-reaction to the scalar hair carried by the black hole at very low temperatures. In this case the area of the black hole horizon shrinks as the temperature is lowered and the system no longer has finite zero-temperature entropy. This was shown in [31] for asymptotically AdS black holes with hair and we have obtained analogous results in our $z > 1$ model with scalar matter included [32]. The scalar hair corresponds to having a charged superfluid condensate in the dual theory and the instability to developing superfluidity bears out

the general expectation that scale invariant quantum critical matter is never found as the true ground state of a system. A further study of the interplay between the heavy fermion physics and superfluidity in these holographic models is an interesting avenue for further work.

We find it intriguing that experimentally measured deviations from Fermi liquid behavior in critically doped heavy fermion alloys can be qualitatively reproduced by holographic duals with Lifshitz symmetry. The curves for $z > 1$ in Figure 4 suggest a power law for C/T at low temperature rather than a logarithm. The experimental data vary from one material to another and both logarithmic and power law fits are used [4]. The fact that our curves for $z > 1$ approach straight lines at low T should not be over interpreted but it is encouraging to see the right trend coming from simple gravitational models with Lifshitz scaling.

Acknowledgments

This work was supported in part by the Göran Gustafsson foundation, the Swedish Research Council (VR), the Icelandic Research Fund, the University of Iceland Research Fund, and the Eimskip Research Fund at the University of Iceland. We thank E. Ardonne, H. Hansson, and P. Kakashili for useful discussions.

References

- [1] H.v. Löhneysen, T. Pietrus, G. Portisch, H.G. Schlager, A. Schröder, M. Sieck, and T. Trappmann, “Non-Fermi Liquid Behavior in a Heavy-Fermion Alloy at a Magnetic Instability,” *Physical Review Letters* **72** 3262 (1994).
- [2] H.v. Löhneysen, M. Sieck, O. Stockert, and M. Waffenschmidt, “Investigation of non-Fermi-liquid behavior in $\text{CeCu}_{6-x}\text{Au}_x$,” *Physica B* **223-224** 471 (1996).
- [3] G. R. Stewart, “Heavy-fermion systems,” *Rev. Mod. Phys.* **56**, 755 (1984).
- [4] G. R. Stewart, “Non-Fermi-liquid behavior in d- and f-electron metals,” *Rev. Mod. Phys.* **73**, 797 (2001) [Addendum-*ibid.* **78**, 743 (2006)].
- [5] H. v. Lohneysen, A. Rosch, M. Vojta and P. Wolfle, “Fermi-liquid instabilities at magnetic quantum phase transitions,” *Rev. Mod. Phys.* **79**, 1015 (2007).
- [6] P. Coleman and A.J. Schofield, “Quantum criticality,” *Nature* **433** (2005) 226 [arXiv:cond-mat/0503002].
- [7] S. A. Hartnoll, “Lectures on holographic methods for condensed matter physics,” *Class. Quant. Grav.* **26**, 224002 (2009) [arXiv:0903.3246 [hep-th]].
- [8] C. P. Herzog, “Lectures on Holographic Superfluidity and Superconductivity,” *J. Phys. A* **42**, 343001 (2009) [arXiv:0904.1975 [hep-th]].

- [9] G. T. Horowitz, “Introduction to Holographic Superconductors,” arXiv:1002.1722 [hep-th].
- [10] J. McGreevy, “Holographic duality with a view toward many-body physics,” arXiv:0909.0518 [hep-th].
- [11] S. Sachdev, “Condensed matter and AdS/CFT,” arXiv:1002.2947 [hep-th].
- [12] J. M. Maldacena, “The large N limit of superconformal field theories and supergravity,” Adv. Theor. Math. Phys. **2**, 231 (1998) [Int. J. Theor. Phys. **38**, 1113 (1999)] [arXiv:hep-th/9711200].
- [13] Q. Si, S. Rabello, K. Ingersent and J.L. Smith, “Locally critical quantum phase transitions in strongly correlated metals,” Nature **413**, 804 (2001).
- [14] S. Kachru, X. Liu, and M. Mulligan, “Gravity Duals of Lifshitz-like Fixed Points,” Phys. Rev. D **78** (2008) 106005 [arXiv:0808.1725 [hep-th]].
- [15] P. Koroteev and M. Libanov, “On existence of Self-Tuning Solutions in Static Braneworlds without Singularities,” JHEP **0802**, 104 (2008) [arXiv:0712.1136 [hep-th]].
- [16] U. H. Danielsson and L. Thorlacius, “Black holes in asymptotically Lifshitz spacetime,” JHEP **0903**, 070 (2009) [arXiv:0812.5088 [hep-th]].
- [17] E. J. Brynjolfsson, U. H. Danielsson, L. Thorlacius and T. Zingg, “Holographic Superconductors with Lifshitz Scaling,” J. Phys. A **43** (2010) 065401 [arXiv:0908.2611 [hep-th]].
- [18] S. J. Rey, “String Theory On Thin Semiconductors: Holographic Realization of Fermi Points and Surfaces,” Prog. Theor. Suppl. **177**, 128 (2009) [arXiv:0911.5295 [hep-th]].
- [19] H. Liu, J. McGreevy and D. Vegh, “Non-Fermi liquids from holography,” arXiv:0903.2477 [hep-th].
- [20] T. Faulkner, H. Liu, J. McGreevy and D. Vegh, “Emergent quantum criticality, Fermi surfaces, and AdS₂,” arXiv:0907.2694 [hep-th].
- [21] M. Taylor, “Non-relativistic holography,” arXiv:0812.0530 [hep-th].
- [22] M. Cubrovic, J. Zaanen, and K. Schalm, “String Theory, Quantum Phase Transitions, and the Emergent Fermi Liquid,” Science **325** (2009) 439.
- [23] S. S. Gubser, I. R. Klebanov and A. M. Polyakov, “Gauge theory correlators from non-critical string theory,” Phys. Lett. B **428**, 105 (1998) [arXiv:hep-th/9802109].
- [24] E. Witten, “Anti-de Sitter space and holography,” Adv. Theor. Math. Phys. **2**, 253 (1998) [arXiv:hep-th/9802150].

- [25] S. A. Hartnoll and P. Kovtun, “Hall conductivity from dyonic black holes,” *Phys. Rev. D* **76**, 066001 (2007) [arXiv:0704.1160 [hep-th]].
- [26] D. W. Pang, “On Charged Lifshitz Black Holes,” *JHEP* **1001**, 116 (2010) [arXiv:0911.2777 [hep-th]].
- [27] G. Bertoldi, B. A. Burrington and A. Peet, “Black Holes in asymptotically Lifshitz spacetimes with arbitrary critical exponent,” *Phys. Rev. D* **80** (2009) 126003 [arXiv:0905.3183 [hep-th]].
- [28] S. F. Ross and O. Saremi, “Holographic stress tensor for non-relativistic theories,” *JHEP* **0909**, 009 (2009) [arXiv:0907.1846 [hep-th]].
- [29] S. A. Hartnoll, J. Polchinski, E. Silverstein and D. Tong, “Towards strange metallic holography,” *JHEP* **1004**, 120 (2010) [arXiv:0912.1061 [hep-th]].
- [30] G. Bertoldi, B. A. Burrington and A. W. Peet, “Thermodynamics of black branes in asymptotically Lifshitz spacetimes,” *Phys. Rev. D* **80**, 126004 (2009) [arXiv:0907.4755 [hep-th]].
- [31] G. T. Horowitz and M. M. Roberts, “Zero Temperature Limit of Holographic Superconductors,” *JHEP* **0911**, 015 (2009) [arXiv:0908.3677 [hep-th]].
- [32] E. J. Brynjolfsson, U. H. Danielsson, L. Thorlacius and T. Zingg, “Holographic models with anisotropic scaling,” arXiv:1004.5566 [hep-th].